

# Downward transfer of momentum by wind-driven waves

Peter Nielsen\*, David P. Callaghan, Tom E. Baldock

School of Civil engineering, The University of Queensland, Brisbane 4072, Australia

## ARTICLE INFO

### Article history:

Received 9 March 2011

Received in revised form 30 June 2011

Accepted 30 June 2011

Available online 29 July 2011

### Keywords:

Wind waves

Wave growth

Reynolds stresses

Wind stress

Dispersion relation

## ABSTRACT

A model for the downward transfer of wind momentum is derived for growing waves. It is shown that waves, which grow due to an uneven pressure distribution on the water surface or a wave-coherent surface shear stress have horizontal velocities out of phase with the surface elevation. Further, if the waves grow in the  $x$ -direction, while the motion is perhaps time-periodic at any fixed point, the Reynolds stresses associated with the organized motion are positive. This is in agreement with several field and laboratory measurements which were previously unexplained, and the new theory successfully links measured wave growth rates and measured sub-surface Reynolds stresses. Wave coherent air pressure (and/or surface shear stress) is shown to change the speed of wave propagation as well as inducing growth or decay. From air pressure variations that are in phase with the surface elevation, the influence on the waves is simply a phase speed increase. For pressure variations out of phase with surface elevation, both growth (or decay) and phase speed changes occur. The theory is initially developed for long waves, after which the velocity potential and dispersion relation for linear waves in arbitrary depth are given. The model enables a sounder model for the transfer to storm surges or currents of momentum from breaking waves in that it does not rely entirely on ad-hoc turbulent diffusion. Future models of atmosphere–ocean exchanges should also acknowledge that momentum is transferred partly by the organized wave motion, while other species, like heat and gasses, may rely totally on turbulent diffusion. The fact that growing wind waves do in fact not generally obey the dispersion relation for free waves may need to be considered in future wind wave development models.

© 2011 Elsevier B.V. All rights reserved.

## 1. Introduction

In waves which propagate with constant form, the horizontal water velocity  $\bar{u}$  is in phase with the surface elevation  $\eta$  and such waves generate no Reynolds stresses for downward momentum transfer because horizontal and vertical velocities are in quadrature, i.e.,  $\overline{u'w'} \equiv 0$ . See e.g., Nielsen (2009) p 5 resp p 33. Reynolds stresses, where they occur, transfer horizontal momentum downwards in the water column, which is instrumental for driving ocean currents and/or storm surges. In the absence of Reynolds stresses, the only avenue for substantial downward momentum transfer would be turbulent diffusion:

$$\tau = \rho \nu_t \frac{\partial \bar{u}}{\partial z} = -\rho \overline{u'w'} \quad (1)$$

where we are using the notation  $u(t) = \bar{u} + \tilde{u} + u'$  to distinguish, steady, periodic and random velocity components.

Waves, even irrotational waves, with  $\overline{u'w'} \neq 0$  are however quite common. Most familiar are probably standing and partially standing waves where non-zero Reynolds stresses drive steady circulation cells half a wave length long, see, e.g., Carter et al. (1973). Less well known

perhaps is the fact that in waves, which grow or decay in say the  $x$ -direction, at constant depth, the organized vertical and horizontal velocities are not in quadrature and hence,  $\overline{u'w'} \neq 0$ . The case of long waves in constant depth decaying due to breaking was described in detail by Deigaard and Fredsøe (1989). Simple, growing (or decaying) waves also have a phase lag (lead) of  $\tilde{u}$  compared with the surface elevation  $\eta$ . Cavaleri and Zecchetto (1987) measured both this  $\tilde{u}$ - $\eta$ -phase lag and  $\overline{u'w'} \neq 0$  in waves that were exposed to strong wind in the field. However, no explanation was offered at the time, probably because no suitable wave theory was at hand (Cavaleri pers com 2011). That is, while several authors, e.g., Miles (1957), Kinsman (1965), Phillips (1966), Young (1999) and Holthuijsen (2007) present theories for why the wind over the ocean should generate an uneven pressure distribution on the water surface, none give a simple explanation for why this should in turn generate  $\tilde{u}$ - $\eta$ -phase lags and  $\overline{u'w'} < 0$  as measured in several field and laboratory experiments. It is clear however that a mechanism, such as  $\overline{u'w'} < 0$  is required in order to distribute wind momentum and energy downwards in the water column in order for the waves and storm surges to grow.

In the following, we offer an explanation in terms of long waves that are growing due to an uneven pressure distribution on the surface. Under certain simplifying assumptions, e.g., sinusoidal shape, the growth rate is found to be exponential if the amplitude of the pressure variation is proportional to the wave amplitude. This is in reasonable agreement with observations as shown by Holthuijsen (2007) p 180. Miles (1957) also found exponential growth, but expressed in terms of a complex

\* Corresponding author. Tel: +61 7 3365 3510; fax: +61 7 3365 4599.  
E-mail address: [p.nielsen@uq.edu.au](mailto:p.nielsen@uq.edu.au) (P. Nielsen).

wave speed, while the waves were assumed periodic in  $x$  (real-value wave number  $k$ ). Such waves have  $\overline{u\tilde{w}} = 0$ , while they do have a time lag of  $u$  relative to  $\eta$ .

Approaching the problem of wave growth via the simpler case of long waves, where a simple wave equation exists and can be solved, automatically delivers the vector for downwards transfer of momentum, namely a non-zero Reynolds stress,  $\overline{u\tilde{w}} \neq 0$ , due to the oscillatory motion, which was measured by Cavaleri and Zecchetto (1987), see Fig. 1.

To the writers' knowledge, this has not previously been used in wind wave growth models although the insight that  $\overline{u\tilde{w}} \neq 0$ , when the wave height varies in space, is implicit in the work of Deigaard and Fredsøe (1989) and Rivero and Arcilla (1995).

In a more or less steady scenario (quasi-equilibrium), the waves may from time to time break (white-capping) whereby some of the energy associated with the oscillatory motion is dissipated, while the time averaged momentum flux is conserved and can contribute to the generation of storm surge. In the scenario, where the waves have been growing in the downwind direction (while perhaps being time-periodic at fixed points) the Reynolds stresses have distributed the momentum downwards during the growth process, so that the vertical distribution of momentum is no longer totally reliant on more or less ad-hoc turbulent diffusion, see Fig. 2.

An improved understanding of the downward momentum transfer in wind driven waves is clearly needed since several modeling studies using well documented wind fields and measured surge levels, e.g. Stewart et al. (2010), indicate that the momentum transfer corresponding to standard values ( $<0.0025$ ) of the wind stress coefficient (Donelan et al., 2006; Powell et al., 2003) is insufficient to produce the measured surges. If indeed the actual downward momentum fluxes are greater than suggested by standard wind stress coefficients, as indicated by wave growth observations (Belcher and Hunt (1998)) and by the subsurface Reynolds stress measurements of Cavaleri and Zecchetto (1987), a better understanding and predictive capability of storm surges can be achieved. The present theory may be a useful step in this direction.

The paper is organized as follows. Section 2 quantifies the  $\tilde{u} - \eta$ -phase shifts and Reynolds stresses for long waves, which grow exponentially in the  $x$  direction while remaining time-periodic at a fixed point. In Section 3, we derive a general wave equation for long waves exposed to a varying surface pressure, and explore in detail the special case of water surface and air pressure being phase shifted sinusoids. We find two categories of solutions:  $x$ -periodic waves, which grow uniformly with time and, time-periodic waves, which grow exponentially in the  $x$ -direction (down wind). Section 4 explores the first category and Section 5 the second. We find that both display  $\tilde{u} - \eta$ -phase shifts, but only the latter have  $\overline{u\tilde{w}} \neq 0$ . Section 6 is a discussion

in terms of wave growth data from Peirson and Garcia (2008) and Reynolds stress data from Cavaleri and Zecchetto (1987). The Appendix extends the shallow water model, giving the velocity potential and dispersion relation for "sine waves", growing due to non-uniform air pressure (or an equivalent wave coherent surface stress), in arbitrary depth. The equivalence, with respect to wave generation, of a surface stress shifted  $90^\circ$  compared with a wave coherent non-uniform pressure, was pointed out by Longuet-Higgins (1969) for sine waves and generalized to arbitrary wave shapes by Nielsen (2009) p 17.

## 2. Reynolds stresses in a simple $x$ -growing wave

Consider a "sine wave", which is growing exponentially in the  $x$ -direction, due to for example wind shear stress and/or uneven pressure on the surface, but which is time-periodic at any fixed point:

$$\eta(x, t) = A_0 e^{\alpha x} \cos k(x-ct) = A_0 e^{\alpha x} \text{Re}\{e^{ik(x-ct)}\} = A_0 \text{Re}\{e^{\alpha x + ik(x-ct)}\} \quad (2)$$

where  $\alpha$ ,  $c$  and  $k$  are all real-valued. We will sometimes omit the "Re" for expediency, i.e., simply write

$$\eta(x, t) = A_0 e^{\alpha x + ik(x-ct)} \quad (3)$$

while it is understood that only the real part

$$\eta = A_0 e^{\alpha x} \cos k(x-ct) \quad (4)$$

has physical meaning.

### 2.1. Horizontal velocities in time periodic, $x$ -growing waves

Starting with the shallow water case, which is simple while qualitatively representative, the horizontal velocities are obtained from the simple continuity equation:

$$\frac{\partial \eta}{\partial t} = -\frac{\partial q}{\partial x} = -h \frac{\partial \tilde{u}}{\partial x} \quad (5)$$

which, with  $\eta$  given by Eq. (3) becomes

$$\frac{\partial \tilde{u}}{\partial x} = -\frac{1}{h} \frac{\partial}{\partial t} A_0 e^{\alpha x + ik[x-ct]} = \frac{1}{h} ikc A_0 e^{\alpha x + ik(x-ct)} \quad (6)$$

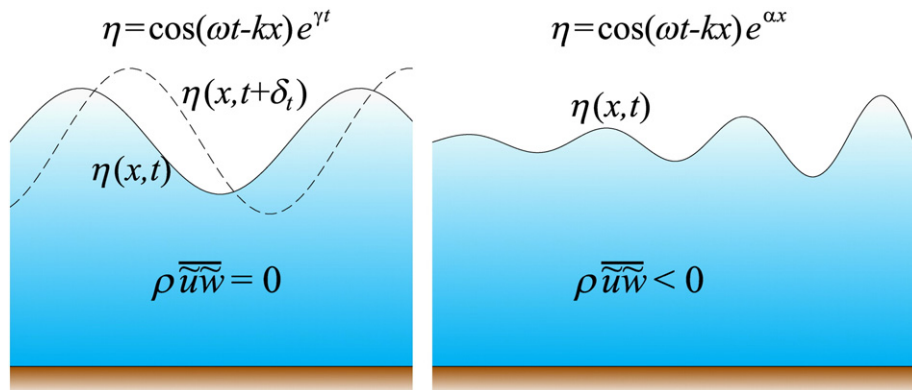
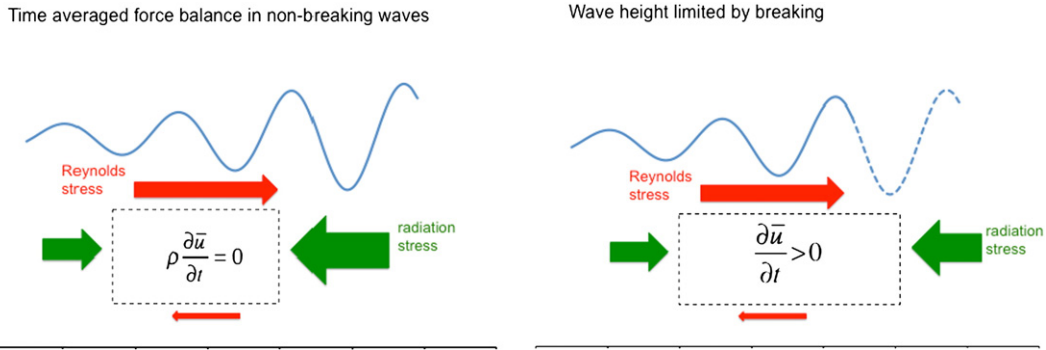


Fig. 1. In waves which grow uniformly in space (left), vertical and horizontal water particle velocities are in quadrature and deliver no Reynolds stresses. In waves, which grow (or decay) in the  $x$  direction, there is a downward transfer of  $x$ -momentum due to Reynolds stresses associated with the organized wave motion.



**Fig. 2.** In waves that grow in the down-wind direction,  $x$ -momentum is transferred downwards by Reynolds stresses as the waves grow. If the wave growth is not limited (left hand scenario) there can be a balance between radiation stress, locally  $\rho \bar{u}^2$ , and the Reynolds stress. If the waves are limited by breaking (right hand scenario) at the down-wind side, the Radiation stress is reduced on that side and part of the “wave-momentum” becomes ocean current. Wind and wave propagation are from left to right.

and by  $\int dx$

$$\begin{aligned} \tilde{u} &= \frac{ik}{\alpha + ik} \frac{cA_0}{h} e^{\alpha x + ik(x-ct)} = \frac{1}{1-i\frac{\alpha}{k}} \frac{cA_0}{h} e^{\alpha x + ik(x-ct)} \\ &= \frac{cA_0}{h\sqrt{1 + \frac{\alpha^2}{k^2}}} e^{\alpha x + ik(x-ct)} e^{i \tan^{-1}(\alpha/k)} \\ &= \frac{cA_0}{h\sqrt{1 + \frac{\alpha^2}{k^2}}} e^{\alpha x + ik\left(x-c\left[t - \frac{1}{kc} \tan^{-1}\frac{\alpha}{k}\right]\right)} \end{aligned} \quad (7)$$

or

$$\tilde{u} = \frac{cA_0 e^{\alpha x}}{h\sqrt{1 + \frac{\alpha^2}{k^2}}} \cos\left[k\left(x-c\left[t - \frac{1}{kc} \tan^{-1}\frac{\alpha}{k}\right]\right)\right] \quad (8)$$

which, by comparison with Eq. (4), shows that for  $x$ -growing waves, there is a time lag of  $\tilde{u}$  relative to  $\eta$ , of magnitude

$$\delta_{t,\eta-u} = \frac{1}{kc} \tan^{-1} \frac{\alpha}{k} \xrightarrow{\alpha/k \rightarrow 0} \frac{\alpha}{k^2 c} \quad (9)$$

while the steady long wave result  $\tilde{u} = \frac{\eta}{h} c$  is recovered for  $\alpha = 0$ .

Cavaleri and Zecchetto (1987), measuring in waves exposed to strong wind, found corresponding phase lags  $\varphi_{\eta u} \approx 35^\circ$  for frequencies up to 0.23 Hz and  $\varphi_{\eta u}$  growing towards  $60^\circ$  for frequencies approaching 0.25 Hz see their Fig. 5. These very substantial phase shifts which correspond to  $\alpha \approx k$  and, in some cases, even  $\alpha > k$  definitely call for further theoretical and experimental investigation.

For decaying waves, which correspond to  $\alpha < 0$ , the corresponding phase-lead of  $\tilde{u}$  over  $\eta$  is well known as for the decaying tidal oscillations shown by Dronkers (1964) p173.

### 2.2. Vertical velocities

The vertical velocities can now be obtained from the horizontal ones via the local continuity equation

$$\frac{\partial \tilde{u}}{\partial x} + \frac{\partial \tilde{w}}{\partial z} = 0 \quad (10)$$

with  $\tilde{w} = 0$  at the impermeable bed,  $z = 0$ , i.e:

$$\begin{aligned} \tilde{w} &= \int_0^z -\frac{\partial \tilde{u}}{\partial x} dz = -\int_0^z \frac{\partial}{\partial x} \left( \frac{ikc}{(\alpha + ik)h} A_0 e^{\alpha x + ik(x-ct)} \right) dz \\ &= -\frac{ikcz}{h} A_0 e^{\alpha x + ik(x-ct)} = -\frac{ikcz}{h} \eta \end{aligned} \quad (11)$$

or in terms of real-valued functions

$$\tilde{w} = -kc \frac{z}{h} A_0 \sin k(x-ct) \quad (12)$$

The  $90^\circ$  phase lead of  $\tilde{w}$  over  $\eta$  indicated by these results, by comparing with Eq. (4), corresponds to the situation in free sine waves and was almost matched by the data of Cavaleri and Zecchetto (1987). They measured a fairly consistent lead of  $80^\circ$ .

### 2.3. Reynolds stresses in time periodic, $x$ -growing waves

The (time averaged) Reynolds stresses can now be evaluated from the above expressions for  $\tilde{u}$  and  $\tilde{w}$ :

$$\begin{aligned} -\rho \overline{\tilde{u} \tilde{w}} &= -\rho \frac{c}{h} A_0 e^{\alpha x} \cos\left(k[x-ct] - \tan^{-1}\frac{\alpha}{k}\right) \left(-\frac{z}{h} kc A_0 e^{\alpha x} \sin k(x-ct)\right) \\ &= \frac{\rho kc^2 A_0^2 e^{2\alpha x} z}{2h^2} \sin\left(\tan^{-1}\frac{\alpha}{k}\right) \approx \frac{\rho \alpha c^2 A_0^2 e^{2\alpha x} z}{2h^2} \text{ for } \alpha \ll k \end{aligned} \quad (13)$$

that is, in a growing wave of the form (3), the organized motion generates a downward flux of horizontal momentum as observed by Shonting (1970) and Cavaleri and Zecchetto (1987) and others in waves exposed to strong following wind. If the waves are decaying due to surface wind stress and/or air pressure, these stresses simply change signs with  $\alpha$ . For a thorough discussion of this case see Deigaard and Fredsøe (1989). If the dissipation is due to bottom friction, the Reynolds stress is maximum at the bed (at the top of the bottom boundary layer), decaying to zero at the surface, balancing the decay of the radiation stress in the  $x$ -direction in analogy with the growth scenario in Fig. 1, left hand panel.

We will show in the following section that the speed of the growing waves is different from the free-wave speed. However, the differences are small enough that the long wave expression, using  $c = \sqrt{gh}$ ,

$$-\overline{\tilde{u} \tilde{w}} = \frac{gH^2(x)z}{2h} \alpha \quad (14)$$

is a useful long-wave approximation.

The dispersion relation for growing waves and Reynolds stress formulae for arbitrary depth are given in the Appendix.

### 3. Waves growing due to non-uniform surface pressure

We will now derive a wave equation for linear long waves of arbitrary shape, acted upon by an uneven surface pressure. Subsequently, considering the special case of sinusoid surface elevation and pressure variation, we show that there are solutions, which exhibit the features measured by Shonting (1970) and by Cavaleri and Zecchetto (1987), namely a phase lag of  $\tilde{u}$  behind  $\eta$  and  $\tilde{u}\tilde{w} < 0$ . To this end, consider the scenario in Fig. 3.

#### 3.1. Waves of arbitrary shape

A long-wave equation for this scenario can be derived from Newton II and the Continuity equation in the same way as the usual linear long wave equation is derived see, e.g. Nielsen (2009) p 6. That is:

$$\text{Newton II gives } \rho \frac{\partial u}{\partial t} = -\rho g \frac{\partial \eta}{\partial x} - \frac{\partial p_a}{\partial x} \quad (15)$$

$$\text{While Continuity gives } \frac{\partial \eta}{\partial t} = -h \frac{\partial u}{\partial x} \quad (16)$$

and between these,  $u$  is eliminated, to give

$$\frac{\partial^2 \eta}{\partial t^2} = gh \frac{\partial^2 \eta}{\partial x^2} + \frac{h}{\rho} \frac{\partial^2 p_a}{\partial x^2}. \quad (17)$$

Both transient and steady solutions to this equations have been explored in Nielsen (2009) pp 16, 151 for arbitrary  $p_a$ -shapes. For the present case of a pressure field which travels with the wave speed, Nielsen's resonant solution (p 23) for arbitrary pressure shape, but constant pressure-strength, gives time-linear wave growth.

#### 3.2. Sine waves exposed to sinusoid pressure

For the purpose of getting the simplest possible illustration of the observed  $\tilde{u} - \eta$ -phase shifts, and finite Reynolds stresses,  $u \neq 0$ , we shall consider a less general scenario, namely, that where both surface elevation and air pressure are sinusoids as in the figure below, and the surface pressure is proportional to the wave amplitude. In that case we have

$$p_a = \frac{P_0}{A_0} e^{ik\delta} \eta \quad (18)$$

so, after assuming sinusoids, the wave Eq. (16) can be written

$$\frac{\partial^2 \eta}{\partial t^2} = gh \left( 1 + \frac{P_0}{\rho g A_0} e^{ik\delta} \right) \frac{\partial^2 \eta}{\partial x^2} \quad (19)$$

which becomes the well known linear long wave equation for free waves, when  $P_0 = 0$ .

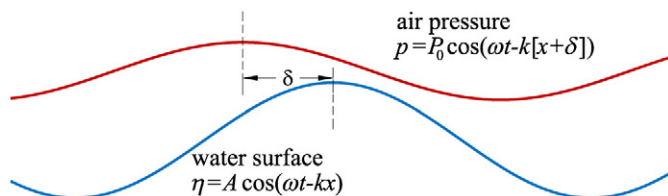


Fig. 3. Sine wave growing due to sinusoid air pressure which peaks up-wind of the crest. The waves propagate from left to right.

The present formulation relates to the sheltering parameter  $S$  of Jeffreys (1925) by  $P_0 = kA_0\rho_{\text{air}}U_r^2S$  and  $\delta = L/4$ , where  $U_r$  is the wind speed relative to the wave form. With the present formulation, Phillips' normalized growth parameter is  $\beta = \frac{P_0 \sin k\delta}{\rho_{\text{air}}U_r^2kA}$ , see e.g. Young (1999), pp 49–50.

For  $P_0 > 0$ , the character of the solutions to Eq. (19) depends on  $\delta$ . That is, for  $\delta = 0$ , there are steady solutions analogous to the free long waves but propagating with the enhanced speed  $\sqrt{gh \left( 1 + \frac{P_0}{\rho g A_0} \right)}$ .

This reflects the fact that a pressure distribution, which peaks at the wave crest, does no work on the water surface and hence doesn't make the waves grow. It does however make the waves propagate faster because it is equivalent to a "stiffening of the water surface" by applying a larger restoring force. See Lighthill (1978), p 223 for the analogous speed increase due to surface tension.

For  $\delta > 0$ , i.e., with the pressure peaking up-wind of the wave crest, there are two kinds of growing solutions, namely:

Time-periodic waves, which grow in the  $x$ -direction:  $\eta(x, t) = A_0 e^{\alpha x} \cos k(x - ct)$  and,  $x$ -periodic solutions which grow uniformly with time:  $\eta(x, t) = A_0 e^{\text{Im}(c)t} \cos k(x - \text{Re}\{c\}t)$ . Miles (1957) and subsequent authors chose to consider the latter form, which perhaps explains that Cavaleri et al's Reynolds stress observations have remained unexplained because these waves have  $\tilde{u}\tilde{w} \equiv 0$ .

For  $\delta < 0$  there are analogous decaying solutions. The quantitative details are given in the following.

#### 4. x-periodic waves growing exponentially with time

First we consider solutions to Eq. (18), which grow with time, but are periodic in the  $x$ -direction and find that while  $u$  lags behind  $\eta$ , there are no wave related Reynolds stresses.

Eq. (18) has  $x$ -periodic solutions of the form

$$\eta(x, t) = A_0 e^{ik \left( x \pm \sqrt{gh \left( 1 + \frac{P_0}{\rho g A_0} e^{ik\delta} \right)} t \right)} \quad (20)$$

of which the one that propagates in the positive  $x$ -direction can be expressed in terms of real-valued functions as

$$\begin{aligned} \eta(x, t) &= A_0 \cos \left( k \left[ x - \text{Re} \left\{ \sqrt{gh \left( 1 + \frac{P_0}{\rho g A_0} e^{ik\delta} \right)} t \right\} \right] \right) e^{k \text{Im} \left\{ \sqrt{gh \left( 1 + \frac{P_0}{\rho g A_0} e^{ik\delta} \right)} t \right\}} \\ &= A_0 \cos(k[x - \text{Re}\{c\}t]) e^{k \text{Im}(c)t} \end{aligned} \quad (21)$$

##### 4.1. Horizontal water particle velocities in x-periodic, growing sine waves

The horizontal water particle velocities corresponding to this wave motion can be derived from the long-wave continuity equation, i.e.,

$$\begin{aligned} \tilde{u} &= -\frac{1}{h} \int \frac{\partial \eta}{\partial t} dx = -\frac{1}{h} \int \frac{\partial}{\partial t} A_0 e^{ik \left( x - \sqrt{gh \left( 1 + \frac{P_0}{\rho g A_0} e^{ik\delta} \right)} t \right)} dx \\ &= -\frac{1}{ik h} \left( -ik \sqrt{gh \left( 1 + \frac{P_0}{\rho g A_0} e^{ik\delta} \right)} \right) A_0 e^{ik \left( x - \sqrt{gh \left( 1 + \frac{P_0}{\rho g A_0} e^{ik\delta} \right)} t \right)} \\ &= \frac{\sqrt{gh \left( 1 + \frac{P_0}{\rho g A_0} e^{ik\delta} \right)}}{h} A_0 e^{ik \left( x - \sqrt{gh \left( 1 + \frac{P_0}{\rho g A_0} e^{ik\delta} \right)} t \right)} = \frac{c}{h} \eta \end{aligned} \quad (22)$$

from which the usual expression for steady long waves  $\tilde{u} = \sqrt{\frac{g}{h}} \eta$  is recovered for  $P_0 = 0$ , while  $P_0, \delta > 0$  leads to a time lag of  $\tilde{u}$  behind  $\eta$ .

#### 4.2. Vertical water particle velocities in $x$ -periodic, growing sine waves

The vertical water particle velocities  $\tilde{w}(x, z, t)$  are derived from  $\tilde{u}(x, z, t)$  through the continuity equation  $\frac{\partial \tilde{u}}{\partial x} + \frac{\partial \tilde{w}}{\partial z} = 0$ . We find

$$\begin{aligned} \tilde{w} &= -\int \frac{\partial \tilde{u}}{\partial x} dz = -\int \frac{\partial}{\partial x} \frac{\sqrt{gh \left(1 + \frac{P_0}{\rho g A_0} e^{ik\delta}\right)}}{h} A_0 e^{ik \left(x - \sqrt{gh \left(1 + \frac{P_0}{\rho g A_0} e^{ik\delta}\right)} t\right)} dz \\ &= ik \sqrt{gh \left(1 + \frac{P_0}{\rho g A_0} e^{ik\delta}\right)} \frac{z}{h} \eta. \end{aligned} \quad (23)$$

#### 4.3. Reynolds stresses in $x$ -periodic, growing sine waves

For these waves  $\tilde{u}$  and  $\tilde{w}$  are seen to be in quadrature,  $\tilde{w} \propto i\tilde{u}$ , so  $\tilde{u}\tilde{w} = 0$ , as indicated by Fig. 1. This is consistent with Rivero and Arcilla (1995) who found that, non-zero Reynolds stresses require spatial variation of the wave amplitude at constant depth.

### 5. Time periodic sine waves growing in the $x$ -direction

We now seek solutions to the wave equation

$$\frac{\partial^2 \eta}{\partial t^2} = gh \left(1 + \frac{P_0}{\rho g A_0} e^{ik\delta}\right) \frac{\partial^2 \eta}{\partial x^2} \quad (19)$$

which are time-periodic at any fixed point but growing exponentially in the  $x$ -direction, i.e., we seek solutions in the form

$$\eta(x, t) = A_0 e^{\alpha x} e^{ik(x-ct)} \quad (24)$$

where  $\alpha$ ,  $k$  and  $c$  are all real-valued. We find that these display non-zero Reynolds stresses as well as the  $\eta$ - $u$  phase-lag. These are the type of waves observed in a laboratory wind wave flume after a steady state has been reached.

Insertion of the form (24) into Eq. (19) leads to

$$-c^2 = \left(\frac{\alpha}{k} + i\right)^2 gh \left(1 + \frac{P_0}{\rho g A_0} e^{ik\delta}\right) \quad (25)$$

where the growth parameter  $\alpha$  must be determined so that  $c$  is real-valued corresponding to time-periodic waves. For the present purposes of qualitative insight, we pursue a simplified solution, corresponding to the practical range  $\alpha \ll k$  in which case we have

$$c^2 \approx \left(1 - 2i \frac{\alpha}{k}\right) gh \left(1 + \frac{P_0}{\rho g A_0} e^{ik\delta}\right) \quad (26)$$

where  $c$  is real-valued if

$$2 \frac{\alpha}{k} = \frac{\frac{P_0}{\rho g A_0} \sin k\delta}{1 + \frac{P_0}{\rho g A_0} \cos k\delta}. \quad (27)$$

That is

$$\alpha = \frac{k}{2} \frac{\frac{P_0}{\rho g A_0} \sin k\delta}{1 + \frac{P_0}{\rho g A_0} \cos k\delta} \xrightarrow{P_0 \rightarrow 0} \frac{k}{2} \frac{P_0}{\rho g A_0} \sin k\delta. \quad (28)$$

So, wind generated uneven air pressure may make sine waves grow in accordance with  $\eta(x, t) = A_0 e^{\alpha x} e^{ik(x-ct)}$  and, we showed in Section 2 that, waves with this form have a phase lag of  $\tilde{u}$  behind  $\eta$  and have  $\tilde{u}\tilde{w} < 0$  as measured in both field and laboratory experiments with waves exposed to following winds. This result can be re-written

in the formulations of Jeffreys (1925) and Miles (1957) as detailed below Eq. (19).

### 6. Discussion

The theory for  $x$ -growing waves brings experimental data on wave growth rates and on sub-surface Reynolds stresses nicely together, while the agreement is less perfect when simultaneous measurements of Reynolds stresses and  $\eta$ - $u$  phase lags are compared.

#### 6.1. Reconciling growth rates and sub-surface Reynolds stresses

According to Peirson and Garcia (2008) Fig. 6, Miles' normalized wind wave growth parameter  $\beta$ , takes values in the range  $10 < \beta < 107$ , which with

$$\alpha = \frac{\rho_{\text{air}} k^2 U_r^2}{2\rho g} \beta \quad (29)$$

and typical values like  $(\rho_{\text{air}}, k, U_r) = (1.2 \text{ kg/m}^3, 0.1 \text{ m}^{-1}, 15 \text{ m/s})$  gives  $\alpha \approx 0.00014\beta$  and the expected range

$$0.0015 \text{ m}^{-1} < \alpha < 0.015 \text{ m}^{-1} \quad (30)$$

This range includes the, Reynolds stress measurements by Cavaleri and Zecchetto. That is, for the data in their Fig. 6, they found  $-\tilde{u}\tilde{w} \approx 0.03 \text{ m}^2/\text{s}^2$ , which through the long-wave approximation (14) corresponds to

$$\alpha = \frac{2h}{H_{\text{rms}}^2 g z} (-\tilde{u}\tilde{w}) = \frac{2 \times 16}{1.4^2 \times 9.8 \times 12} 0.03 = 0.0042 \text{ m}^{-1} \quad (31)$$

For comparison, the corresponding deep water expression, with  $z'$  measured from the mean surface level, using the deep water free-wave speed:  $c_0 = \frac{gT}{2\pi}$  gives

$$\begin{aligned} \alpha &= \frac{2e^{-2k_0 z'}}{k_0 H_{\text{rms}}^2 c_0^2} (-\tilde{u}\tilde{w}) = \frac{2e^{-2k_0 z'}}{H_{\text{rms}}^2 g} (-\tilde{u}\tilde{w}) \\ &= \frac{2e^{-2 \times 0.124 \times (-4)}}{1.4^2 \times 9.8} 0.03 = 0.0084 \text{ m}^{-1} \end{aligned} \quad (32)$$

The latter result is the more appropriate since Cavaleri and Zecchetto's experimental conditions,  $(T, h) = (5.7 \text{ s}, 16 \text{ m})$  were almost deep water.

The  $\alpha$ -value can be interpreted in terms of a pressure amplitude  $P_0$  through Eq. (28), e.g:

$$P_0 = \frac{2\rho g A_0 \alpha}{k^2 \delta} = \frac{2 \times 1025 \times 9.8 \times 0.7 \times 0.0086}{0.127} = 952 \text{ Pa} \quad (33)$$

where we have taken  $\delta = L/6$  corresponding to  $k\delta \approx 1$ . A sinusoid surface pressure with these  $(P_0, \delta)$  is, in terms of horizontal force on the surface, equivalent to a uniform surface shear stress of

$$\begin{aligned} \bar{\tau}_w &= \frac{1}{L} \int_{x_0}^{x_0+L} p_a \frac{\partial \eta}{\partial x} dx = \frac{1}{L} \int_{x_0}^{x_0+L} P_0 \cos k(x + \delta) (-k \sin kx) dx \\ &= \frac{1}{2} P_0 \sin k\delta = \frac{1}{2} \times 952 \times \frac{\sqrt{3}}{2} = 412 \text{ Pa}. \end{aligned} \quad (34)$$

In comparison, the wind shear stress corresponding to  $C_{10} = 0.0025$  and  $U_{10} = 15 \text{ m/s}$  is

$$\bar{\tau}_w = \frac{1}{2} \rho_{\text{air}} C_{10} U_{10}^2 = \frac{1}{2} \times 1.2 \times 0.0025 \times 15^2 = 0.34 \text{ Pa} \quad (35)$$

i.e., smaller by a factor 1220!

So, while Cavaleri and Zecchetto's Reynolds stresses are two or three orders of magnitude greater than the estimated wind stresses, they agree, through the present theory, with the wave growth data presented by Peirson and Garcia (2008). This discrepancy between wind shear stresses and wave growth rates has previously been commented upon by van Duin (1996) and by Belcher and Hunt (1998).

6.2. Discrepancies between the theory and observed  $(\varphi_{\eta-u}, \tilde{u}\tilde{w})$  data sets

The data in Fig. 6 of Cavaleri and Zecchetto (1987), indicate that  $\tilde{u}$  lags  $\eta$  by

$$\varphi_{\eta-u} = 1.001 \pm 0.294 \text{ radians} \tag{36}$$

which in terms of growth rates  $\alpha = k\varphi_{\eta-u}$  corresponds to

$$\alpha = 0.13 \pm 0.07. \tag{37}$$

This range for  $\alpha$  disagrees with Eq. (32) and is well above the range reported by Peirson and Garcia (2008). Perhaps Cavaleri and Zecchetto's measurements of  $\eta$  were time-biased due to the surface gage reacting to foam on the front of the waves? However, similar phase differences  $\varphi_{\eta-u} \approx T/6$  are indicated for the decaying tidal wave of Dronkers (1964) p173, and Peirson et al. (2003) measured decay of laboratory waves in opposing wind corresponding to  $\alpha = -0.42$ , see the 15 m/s case in their Fig. 4.

6.3. Future experimental investigations

In order to verify and/or refine the present theory, new experiments should be carried out where details of the sub-surface pressure is measured as well as the surface elevation and the water particle velocities.

6.4. Implications for atmosphere–ocean exchange models

As a first approximation, the transfer between atmosphere and ocean is often quantified in terms of gradient diffusion:

$$\text{Flux}_i = -K_i \times \overrightarrow{\text{grad}}(c_i) \tag{38}$$

for the  $i$ -th species, e g, momentum, heat, CO<sub>2</sub> and other gasses. The simplest hypothesis is then that all species diffuse with the same turbulent diffusion coefficient,  $K_i \equiv K$ , meaning that flux and concen-

tration gradient need only be measured for one species in order to provide all necessary  $K_i$ . However, when one or more species are transferred partly by the organized wave motion, as described above for momentum, different species must be expected to have different diffusion coefficients if their total flux is written in the form of (38).

7. Conclusions

A theory has been provided to explain why waves, exposed to uneven surface pressure (or an equivalent wave coherent shear stress) generated by winds display two important features which are not found in waves that propagate with constant form.

Firstly, if the wind induces an uneven pressure distribution on the water surface, this alters the phase relation between  $\tilde{u}$  and  $\eta$ . If the pressure does positive work on the water surface so that the wave amplitude grows as  $A(x) = A_0 e^{\alpha x}$ ,  $\tilde{u}$  is found to be lagging behind  $\eta$  by the phase angle  $\varphi_{\eta-u} = \alpha/k$  [radians].

Secondly, with  $\tilde{u}$  lagging behind  $\eta$  while  $\tilde{w}$  is in phase with  $\frac{\partial \eta}{\partial t}$ , we find  $\tilde{u}\tilde{w} < 0$ , in agreement with the measurements of Cavaleri and Zecchetto (1987), representing a non-turbulent flux of wind driven momentum downward into the water column. The distribution of these “organized Reynolds stresses” is linear in a long wave, corresponding to the wind momentum being deposited uniformly in the water column. In a deep water wave the distribution will be decaying exponentially downwards on the scale of the wave length.

The wave related Reynolds stresses measured by Cavaleri and Zecchetto (1987), which were, in the absence of relevant theory, previously considered unrealistically large, are shown to fit within the experimental range for wave growth via the present theory.

A quasi-steady sea state can be thought of as a scenario, where the waves alternately grow in accordance with the model above, alternately break (white capping) whereby some of the oscillatory energy is dissipated while the steady momentum flux is conserved. The momentum which, through the white-capping, becomes available to drive currents or storm surge is by this model already distributed through the water column, see Fig. 1, while previous models with  $\tilde{u}\tilde{w} = 0$  had to rely entirely on turbulent diffusion for the downward distribution of this momentum.

For simplicity, the theory was derived in detail for long waves. However, the corresponding velocity potential and dispersion relation for wind-driven “sine waves” at arbitrary depths, which explains the same features, are given in the Appendix.

The fact that wind driven waves in general obey a different dispersion relation from that of free waves, and hence have different, generally complex, wave numbers, may need to be considered in new wind-wave development models.

Acknowledgements

The authors would like to thank Professor Tony Bracken for mathematical guidance and Dr Rolf Deigaard for incisive comments.

Appendix. Wind-driven sine waves in arbitrary depths

A1. The velocity potential

We now seek the velocity potential  $\phi(x, z, t)$  corresponding to the surface form (24):

$$\begin{aligned} \eta(x, t) &= A_0 e^{\alpha x} \cos k(x-ct) \\ &= A_0 e^{\alpha x} \text{Re} \left\{ e^{ik(x-ct)} \right\} \\ &= A_0 \text{Re} \left\{ e^{(\alpha+ik)x - ikct} \right\} \end{aligned} \tag{A1}$$

where  $\alpha$ ,  $k$  and  $c$  are all real-valued.

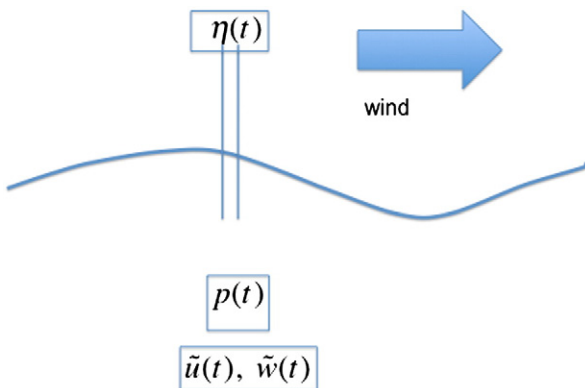


Fig. 4. Suggested new experimental setup where the sub surface pressure is measured as well as the previously measured quantities. From this data, the wind induced, wave-coherent surface pressure can then be inferred from  $p_a(t) \approx p(z_a, t) - \rho g(\eta - z_a)$ . It seems that this procedure is much easier than trying to measure the air pressure just above the water surface.

The velocity potential is tied to  $\eta(x, t)$  through the free surface boundary condition, which in its linearised form, for free waves with uniform air pressure reads.

$$g\eta = \left. \frac{\partial\phi}{\partial t} \right|_{z=\eta} \quad (\text{A2})$$

cf Le Mehaute (1976) p 214 or Lighthill (1978) p208. Replacing  $g$  by  $g\left(1 + \frac{P_0}{\rho g A_0} e^{ik\delta}\right)$  as suggested by Eq. (19) leads to the revised surface condition.

$$g\left(1 + \frac{P_0}{\rho g A_0} e^{ik\delta}\right)\eta = \left. \frac{\partial\phi}{\partial t} \right|_{z=\eta} \quad (\text{A3})$$

and then to the potential.

$$\phi(x, z, t) = \text{Re}\left\{i \frac{g}{kc} \left(1 + \frac{P_0}{\rho g A_0} e^{ik\delta}\right) A_0 e^{(\alpha + ik)x - ikt} f(z)\right\} \quad (\text{A4})$$

where the function  $f(z)$  should be 1 at the water surface and of such a form that  $\phi$  satisfies the Laplace Equation. For deep water the analogy with free sine waves is.

$$\begin{aligned} \phi(x, z, t) &= \text{Re}\left\{i \frac{g}{kc} \left(1 + \frac{P_0}{\rho g A_0} e^{ik\delta}\right) A_0 e^{(\alpha + ik)x} e^{(\alpha + ik)iz} e^{-ikt}\right\} \\ &= \text{Re}\left\{i \frac{g}{kc} \left(1 + \frac{P_0}{\rho g A_0} e^{ik\delta}\right) A_0 e^{(\alpha + ik)(x + iz)} e^{-ikt}\right\} \end{aligned} \quad (\text{A5})$$

where  $z = 0$  at the mean surface level.

For intermediate depths, the analogy with free sine waves gives.

$$\phi(x, z, t) = \text{Re}\left\{i \frac{g}{kc} \left(1 + \frac{P_0}{\rho g A_0} e^{ik\delta}\right) A_0 e^{(\alpha + ik)x} \frac{\cosh[(k - i\alpha)(z + h)]}{\cosh[(k - i\alpha)h]} e^{-ikt}\right\} \quad (\text{A6})$$

and the corresponding water particle velocities given by  $\tilde{u} = -\frac{\partial\phi}{\partial x}$  respectively,  $\tilde{w} = -\frac{\partial\phi}{\partial z}$ .

## A2. The dispersion relation for wind driven waves

The influence of the surface pressure on the wave speed and/or the wave length is analogous to the long wave results inferred from Eq. (19). That is, the relevant dispersion relation is obtained by replacing  $g$  by  $g\left(1 + \frac{P_0}{\rho g A_0} e^{ik\delta}\right)$  in the dispersion relation for free sine waves:

$$k_{\sin} \tanh k_{\sin} h = \frac{\omega^2}{g} \quad (\text{A5})$$

That is, the complex wave number  $k - i\alpha$  for wind driven “sine waves” (ref Fig. 3) is determined from.

$$(k - i\alpha) \tanh(k - i\alpha)h = \frac{\omega^2}{g\left(1 + \frac{P_0}{\rho g A_0} e^{ik\delta}\right)} \quad (\text{A6})$$

For the analogous dispersion relation for waves with significant “surface stiffening” due to surface tension, see e.g. Longuet-Higgins and

Stewart (1964), Eq. (10) or Lighthill (1978), p 226. For the surface tension case, the wave numbers are still real valued ( $\alpha = 0$ ), corresponding to the special case of  $\delta = 0, L/2$  in (A6).

The magnitude of deviations from the free-wave wave numbers depends on the size of  $\frac{P_0}{\rho g A_0} e^{ik\delta}$ , which can be judged from  $\frac{P_0}{\rho g A_0} \sin k\delta = \frac{\rho_{\text{air}} k U_r^2}{\rho g} \beta$  and the experimental range [10;107] for  $\beta$ , Peirson and Garcia (2008) Fig. 6. With typical values like  $(\rho_{\text{air}}, k, U_r) = (1.2\text{kg/m}^3, 0.1\text{m}^{-1}, 15\text{m/s})$  this leads to

$$\frac{P_0}{\rho g A_0} \sin k\delta \in [0.028; 0.29] \quad (\text{A7})$$

The fact that growing waves thus have a different dispersion relation from free waves, and in general have complex wave numbers may need to be incorporated into the next generation of (spectral) wind wave development models.

## References

- Belcher, S.E., Hunt, J.C.R., 1998. Turbulent flow over hills and waves. *Ann. Rev. Fluid Mech.* 30, 507–538.
- Carter, T.G., Liu, P.L.-F., Mei, C.C., 1973. Mass transport by waves and offshore bed-forms. *J. Waterw. Harbours Coast. Div., ASCE* 99, 165–184.
- Cavaleri, L., Zecchetto, S., 1987. Reynolds stresses under wind waves. *J. Geophys. Res.* 92 (No. C4), 3894–3904.
- Deigaard, R., Fredsøe, J., 1989. Shear stress distribution in dissipative water waves. *Coast. Eng.* 13, 357–378.
- Donelan, M.A., Babanin, A.V., Young, I.R., Banner, M.L., 2006. Wave follower field measurements of the wind input spectral function. Part 2, parameterization of wind input. *J. Phys. Oceanogr.* 36, 1672–1689.
- Dronkers, J.J., 1964. *Tidal Computations in Rivers and Coastal Waters*. (North Holland, 518 pp.).
- Holthuijsen, L.H., 2007. *Waves in Oceanic and Coastal Waters*. Cambridge University Press. (387 pp.).
- Jeffreys, H., 1925. On the formation of water waves by wind. *Proc. R. Soc. Lond. A* 107, 189–206.
- Kinsman, B., 1965. *Wind Waves: Their Generation and Propagation on the Ocean Surface*. Prentice Hall, p. 676.
- Le Mehaute, B., 1976. *An Introduction to Hydrodynamics and Water Waves*. Springer. (315 pp.).
- Lighthill, M.J., 1978. *Waves in Fluids*. Cambridge Univ Press. (504 pp.).
- Longuet-Higgins, M.S., 1969. Action of a variable stress at the surface of water waves. *Phys. Fluids* 12 (No. 4), 737–740.
- Longuet-Higgins, M.S., Stewart, R.W., 1964. Radiation stress in water waves; a physical discussion with applications. *Deep Sea Res.* 11, 529–562.
- Miles, J.W., 1957. On the generation of surface waves by shear flows. *J. Fluid Mech.* 3, 185–204.
- Nielsen, P., 2009. *Coastal and Estuarine Processes*. World Scientific. (341 pp.). 978-981-283-711-0 or 978-981-283-712-7 (pbk).
- Peirson, W.L., Garcia, A.W., 2008. On the wind-induced growth of slow water waves of finite steepness. *J. Fluid Mech.* 608, 243–274.
- Peirson, W.L., Garcia, A.W., Pells, S.E., 2003. Water wave attenuation due to opposing wind. *J. Fluid Mech.* 487, 345–365.
- Phillips, O.M., 1966. *Dynamics of the Upper Ocean*. Cambridge University Press. (261 pp.).
- Powell, M.D., Vickery, P.J., Reinhold, T.A., 2003. Reduced drag coefficient for high wind speeds in tropical cyclones. *Nature* 422, 279–283.
- Rivero, F.J., Arcilla, A.S., 1995. On the vertical distribution of  $\overline{u'w'}$ . *Coast. Eng.* 25 (3–4), 137–152.
- Shonting, D.H., 1970. Observations of Reynolds stresses in wind waves. *Pure Appl. Geophys.* 81 (No. 4), 202–210.
- Stewart, J.P., Callaghan, D.P., Nielsen, P., 2010. Tropical Cyclone ‘Roger’ Storm Surge Assessment, School of Civil Engineering Research Report CE162. The University of Queensland, Brisbane.
- van Duin, C., 1996. Rapid distortion turbulence models in the theory of surface wave generation. *J. Fluid Mech.* 329, 147–153.
- Young, I.R., 1999. *Wind Generated Ocean Waves*. Elsevier. (288 pp.).